EJONS International Journal on Mathematic, Engineering and Natural Sciences ISSN 2602 - 4136

Article Arrival Date 03.02.2021 | Article Type Research Article | Article Published Date 20.03.2022

Doi Number: http://dx.doi.org/10.38063/ejons.552

TX ARİ: OLASI BİR ÜÇÜNCÜ BİLEŞENE SAHİP YARI-AYRIK ÖRTEN ÇİFT YILDIZ SİSTEMİ

TX ARI: THE SEMI-DETACHED ECLIPSING BINARY STAR SYSTEM WITH A POSSIBLE THIRD COMPONENT

Oğuz ÖZTÜRK

Arş. Gör. Dr., Çanakkale Onsekiz Mart Üniversitesi, Fen Edebiyat Fakültesi, Fizik Bölümü, Çanakkale/Türkiye.

Arş. Gör. Dr., Çanakkale Onsekiz Mart Üniversitesi, Astrofizik Araştırma Merkezi ve Ulupınar Gözlemevi, Çanakkale/Türkiye. ORCID: 0000-0002-9135-9865

ÖZET

TX Ari örten çift yıldız sistemi birçok gözlem projesi kapsamında gözlenmiş olmasına rağmen, bu örten çift yıldız sistemi üzerine şimdiye kadar detaylı bir fotometrik çalışma henüz yapılmamıştır. TX Ari sisteminin, *V* filtresinde yapılan All-Sky Automated Survey for Supernovae (ASAS-SN) gözlemleri kullanılarak, ışık eğrisinin çözümü ilk defa bu çalışmada sunulmuştur. Çözüm sonucunda sistemin yarı-ayrık bir örten çift yıldız sistemi olduğu sonucuna varılmıştır. Sistemi oluşturan birinci ve ikinci bileşenlerin kütle ve yarıçap değerleri, sırasıyla, $M_1 = 1.85 \pm 0.19$ M⊙, $R_1 = 2.73 \pm 0.19$R⊙ ve $M_2 = 0.44 \pm 0.15$ M⊙, $R_2 = 3.07 \pm 0.47$R⊙ olarak tahmin edilmiştir. TX Ari sisteminin literatürde verilen gözlemleri kullanılarak, sistemin 11 yeni minimum zamanı hesaplanmıştır. Sistemin literatürde yayınlanan minimum zamanları ile birlikte bu çalışmada hesaplanan tüm minimum zamanları kullanılarak, yörünge dönem analizi de ilk defa bu çalışmada sunulmuştur. Yörünge dönem analizinde O-C yöntemi kullanılmıştır. Dönem analizi sonucunda sistemin yörünge döneminin sürekli olarak 0.066 ± 0.013 s/yıl hızı ile artığı tespit edilmiştir. Yörünge dönemindeki bu artış, ikinci bileşenden birinci bileşene korunumlu olmayan kütle aktarımı mekanizması ile açıklanmıştır. Ayrıca sistemin O-C diyagramında, dönemi 17.4 ± 1.3 yıl olan çevrimsel bir değişim tespit edilmiştir. Bu çevrimsel değişimin, sisteme fiziksel olarak bağlı üçüncü bir cisim kaynaklı olduğu kabul edildiğinde üçüncü cismin kütle fonksiyonu $f(M_3) = 0.01249 \pm 0.00028$ M⊙ olarak hesaplanmıştır.

Anahtar Kelimeler: Yıldızlar, örten çift yıldızlar, TX Ari

ABSTRACT

Although eclipsing binary star system TX Ari was observed by several observational missions, there has been no detailed photometric study on the system so far. Using the All-Sky Automated Survey for Supernovae (ASAS-SN) observations of TX Ari, which were made in the V filter, the light curve solution of the system is presented for the first time in this study. As a result of the solution, it was concluded that the system is a semi-detached eclipsing binary star system. The mass and radius values of the primary and secondary components forming the system were estimated as $M_1 = 1.85 \pm 0.19$ M⊙, $R_1 = 2.73 \pm 0.19$ R⊙ and $M_2 = 0.44 \pm 0.15$ M⊙, $R_2 = 3.07 \pm 0.47$R⊙, respectively. Using observations of TX Ari system given in the literature, 11 new minima times of the system were calculated. Orbital period analysis is also presented for the first time in this study, using all the minima times calculated in this study together with the minima times of the system published in the literature. O-C method was used in the orbital period analysis. As a result of the period analysis, it was determined that the orbital period of the system increased continuously with a rate of 0.066 ± 0.013 s/year. This increase in the orbital period is explained by the non-conservative mass transfer mechanism from the secondary component to the primary component. In addition, a cyclical change with a period of 17.4±1.3 years was detected in the O-C diagram of the system. Assuming that the cyclical change is caused by a third body, which is physically bound to the system, the mass function of the third body is calculated as $f(M_3) = 0.01249 \pm 0.00028$ M⊙.

Keywords: Stars, eclipsing binary stars, TX Ari

1. INTRODUCTION

TX Ari (TYC 1795-692-1, Gaia DR2 115966492111381760, 2MASS J03055179+2834400, V=11.49 mag) eclipsing binary star system was classified as an Algol type (EA) eclipsing binary star system by Samus' et al. (2017). This system has been observed within the scope of many observation projects. On the other hand, there has been no detailed photometric study on the system so far. The light curve solution and orbital period analysis of the neglected eclipsing binary star system TX Ari is presented for the first time in this study.

2. OBSERVATIONS

Table 1. Brief information about photometric observations of TX Ari.

Survey	Filter	Start-end date of Observations	Number of observations
		(day/month/year)	
APASS	(B, V, *r*, *g*, *i*, *z*)	02/11/2011.- 04/01/2014	64
ASAS-SN	V	22/11/2013- 29/11/2018	248
CRTS	Unfiltered	29/09/2005.- 24/10/2013	373
KWS	(B, V, Ic)	18/10/2011- 19/01/2021	1241
NSVS	Unfiltered	11/07/1999- 27/03/2000	344
WASP	Broad band (400-700nm)	08/07/2004- 23/07/2008	4526

Some of the observation projects in which the TX Ari system has been observed are: AAVSO Photometric All-Sky Survey (APASS) (Levine et al., 2019), All-Sky Automated Survey for Supernovae (ASAS-SN) (Shappee et al., 2014; Kochanek et al., 2017), Catalina Realtime Transient Survey (CRTS) (Drake et al., 2009), Kamogata/Kiso/Kyoto wide-field survey (KWS) (http://kws.cetus-net.org/~maehara/VSdata.py), Northern Sky Variability Survey (NSVS) (Woźniak et al., 2004) and Wide Angle Search for Planets (WASP) (Butters et al., 2010). Brief information about the observations of the TX Ari system made within the scope of these projects is given in Table 1.

In this study, ASAS-SN (Shappee et al., 2014; Kochanek et al., 2017) observations, which were made in *V* filter, were used as an observational data in the light curve analysis of the system.

3. LIGHT CURVE ANALYSIS

Since there is no spectral study of the TX Ari so far, the effective temperature of the primary component was taken as 7857±324K from Gaia DR2 (Andrae et al., 2018). Before starting the light curve solution, the ASAS-SN observations of the system were phased using the light element obtained in the next section. Wilson-Devinney (WD) software (Wilson & Devinney 1971, Wilson 2012) was used for light curve analysis. Since ASAS-SN observations made in the V filter, the effective wavelength of the filter, where the observations were made, was assumed to be 550 nm. The bolometric gravity-darkening exponents (g_1 and g_2) of the components for a radiative atmosphere ($T > 7200$ K) and for a convective atmosphere ($T < 7200$ K) were taken to be 1.0 and 0.32, respectively (von Zeipel, 1924; Lucy, 1967). The bolometric albedos (A_1 and A_2) of the components were fixed to 1.0 for a radiative atmosphere and 0.5 for a convective atmosphere (Ruciński, 1969). When the analysis was started, the third-body light contribution parameter (l_3) was adjusted as free parameter, but no obvious third-body light contribution was detected. Therefore, the third-body light contribution is neglected in the solution ($l_3 = 0$). Finally, it is assumed that while the component stars revolve around each other in a circular orbit ($e = 0$), they also rotate around themselves synchronously ($F_1 = F_2 = 0$).

The light curve analysis was first started in the detached configuration, i.e., in mode 2. After a few iterations, the solution was continued in the semi-detached configuration (mode 5), as it was seen that the secondary component filled its Roche lobe. During the iterations, phase shift (ϕ), orbital inclination (i), effective temperature of the secondary component (T_2), dimensionless surface gravity of the primary component (Ω_1), mass ratio (q) and luminosity of the primary component (L_1) were chosen as the free parameters. In order to determine the initial value of the mass ratio parameter for the light curve solution, the q- search method was carried out since the spectroscopic mass ratio of the system has not been published in the literature so far. All parameters mentioned above, except the mass ratio, were set as free parameters during the q-search procedure. A diagram of the sum of the squared residuals ($\sum(O-C)^2$) of the light curve models with respect to the related mass ratio values is shown in Figure 1. The initial value of the mass ratio was set to q = 0.22 for the light curve solution since the minimum value of $\sum(O-C)^2$ was achieved at q = 0.22 (see Figure 1).

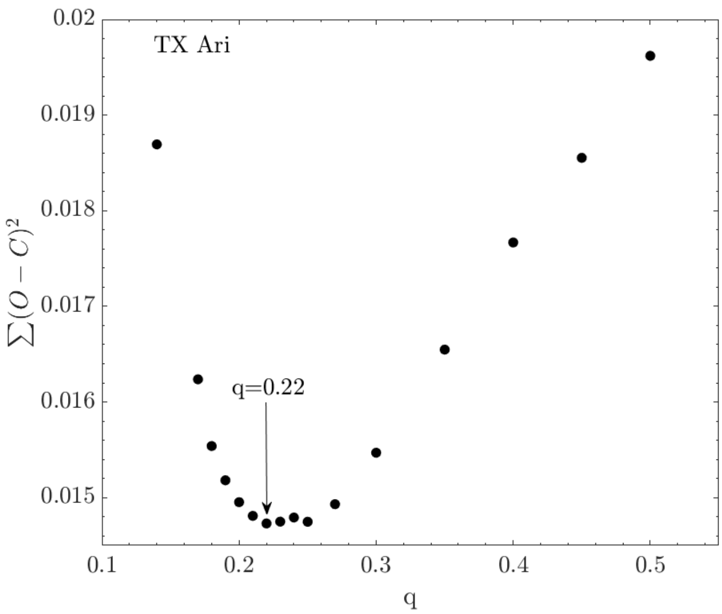

Figure 1. Sum of squared residuals ($\sum(O-C)^2$) versus related mass ratio (q) values of TX Ari.

The light curve parameters obtained from the solution are given in Table 2. The theoretical light curve obtained from the solution together with the light curve obtained from the observations is given in Figure 2. Using the light curve solution parameters given in Table 2, the Roche geometry of the system, obtained with Binary Maker (Bradstreet and Steelman, 2002), is shown in Figure 3.

Table 2. Parameters obtained from best W-D model fit to ASAS-SN light curve of TX Ari.

Parameter	Value
T_0(HJD)*	2452502.1869 ± 0.0099
P(days) *	2.691340 ± 0.000002
ϕ	0.0004 ± 0.0001
i(deg.)	81.6 ± 1.1
T_1(K)	7857
T_2(K)	4022± 101
$q(= M_2/M_1)$	0.239±0.056
Ω_1	4.208±0.021
Ω_2	2.328
r_1 (vol.)	0.254±0.002
r_2 (vol.)	0.286±0.003
L_1	11.927± 0.023
L_2	0.508
$\sum(O-C)^2$	0.0148

*Values obtained from the orbital period analysis of the TX Ari (see Section 3)

As a result of the light curve analysis, it was concluded that the secondary component completely filled its Roche lobe but the primary component filled only 56% of its Roche lobe. Therefore, the system can be classified as a semi-detached binary star system.

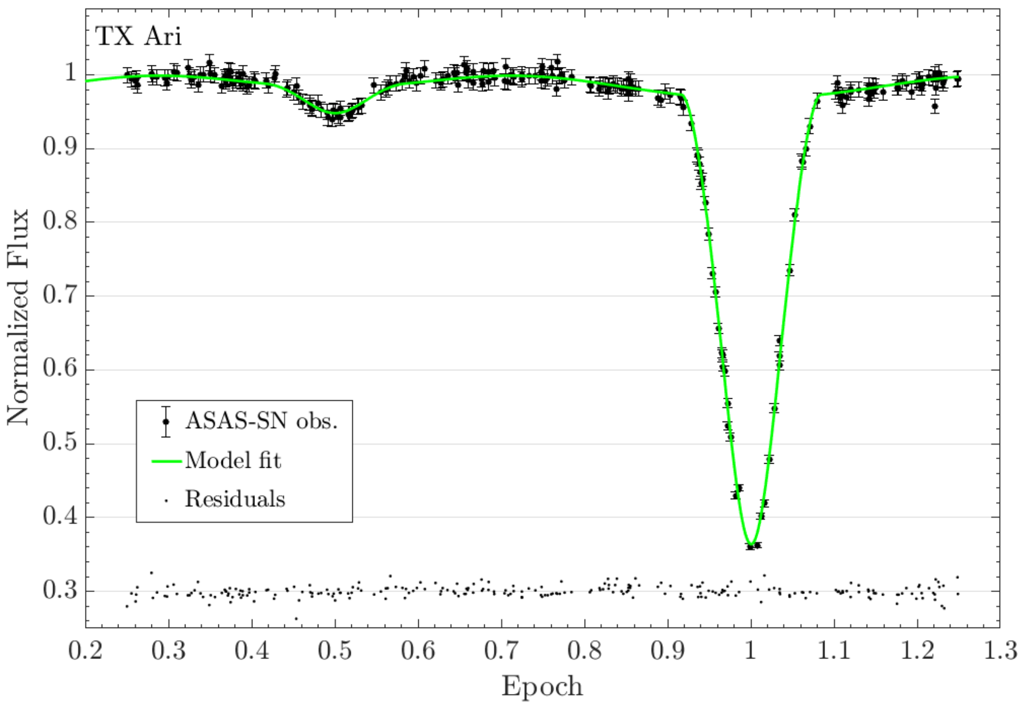

Figure 2. Observed light curve of TX Ari from ASAS-SN observations. Best theoretical fit is illustrated by solid green line. Black dots at bottom of diagram correspond to residuals obtained from the model fit.

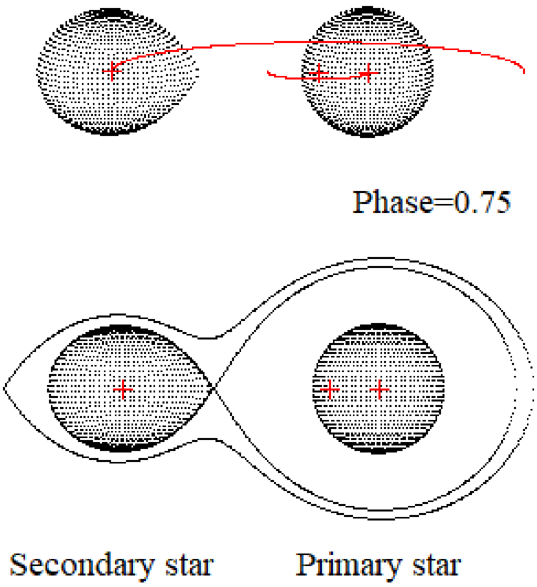

Figure 3. Roche geometry of TX Ari obtained from light curve analysis.

4. ORBITAL PERIOD ANALYSIS

The orbital period analysis of the TX Ari system is first presented in this study.

The number of minima times and references taken from the literature, which are used in the period analysis of the system, are as follows: 45 minima times from O-C Gateway (http://var2.astro.cz/ocgate/) database, 1 minima time from BBSAG Bulletin (2000), 1 minima time from Nelson (2006), 1 minima time from Brát et al. (2009), 1 minima time from Nagai (2008), 1 minima time from Zasche et al. (2011), 1 minima time from Diethelm (2010), 1 minima time from Brát et al. (2011), 1 minima time from Hoňková et al. (2013), 1 minima time from Diethelm (2012a), 1 minima time from Diethelm (2012b), 1 minima time from Hübscher (2017), and 1 minima time from Juryšek et al. (2017). On the other hand, 11 new minima times of the system were calculated in this study from ASAS-SN, KWS and WASP observations. In the orbital period analysis of the TX Ari, all the minima times calculated in this study together with all the minima times taken from the literature were used. The minima times used in the analysis and their references are given in Table 3.

Table 3. Minima times used in the O-C analysis of TX Ari.

Time of minima	Uncertainty	Minima Type	Reference	Remarks
(HJD)				
2428409.54600	-	Min I (photographic)	Gessner (O-C Gateway)	-
2428495.55400	-	Min I (photographic)	Gessner (O-C Gateway)	-
2428783.58900	-	Min I (photographic)	Gessner (O-C Gateway)	-
2429168.50400	-	Min I (photographic)	Gessner (O-C Gateway)	-
2430258.52900	-	Min I (photographic)	Gessner (O-C Gateway)	-
2430998.49700	-	Min I (photographic)	Gessner (O-C Gateway)	-
2431329.57200	-	Min I (photographic)	Gessner (O-C Gateway)	-
2432882.44900	-	Min I (photographic)	Gessner (O-C Gateway)	-
2433178.49000	-	Min I (photographic)	Gessner (O-C Gateway)	-
2433302.32800	-	Min I (photographic)	Gessner (O-C Gateway)	-
2434392.32800	-	Min I (photographic)	Gessner (O-C Gateway)	-
2434599.55500	-	Min I (photographic)	Gessner (O-C Gateway)	-
2434607.54600	-	Min I (photographic)	Gessner (O-C Gateway)	-
2434661.43800	-	Min I (photographic)	Gessner (O-C Gateway)	-
2436160.53800	-	Min I (photographic)	Gessner (O-C Gateway)	-
2436249.30800	-	Min I (photographic)	Gessner (O-C Gateway)	-

2436526.54300	-	Min I (photographic)	Gessner (O-C Gateway)	-
2436822.59700	-	Min I (photographic)	Gessner (O-C Gateway)	-
2436849.51800	-	Min I (photographic)	Gessner (O-C Gateway)	-
2443903.31700	-	Min I (visual)	Locher (O-C Gateway)	-
2444164.38800	-	Min I (visual)	Locher (O-C Gateway)	-
2444581.53300	-	Min I (visual)	Locher (O-C Gateway)	-
2444842.56500	-	Min I (visual)	Locher (O-C Gateway)	-
2444877.50900	-	Min I (visual)	Locher (O-C Gateway)	-
2444993.24400	-	Min I (visual)	Locher (O-C Gateway)	-
2445324.31400	-	Min I (visual)	Mavrofridis (O-C Gateway)	-
2445574.61900	-	Min I (visual)	Locher (O-C Gateway)	-
2445617.68800	-	Min I (visual)	Locher (O-C Gateway)	-
2445698.40700	-	Min I (visual)	Locher (O-C Gateway)	-
2445725.32100	-	Min I (visual)	Locher (O-C Gateway)	-
2446029.37300	-	Min I (visual)	Mavrofridis (O-C Gateway)	-
2446306.64000	-	Min I (visual)	Locher (O-C Gateway)	-
2447111.35900	-	Min I (visual)	Blaettler (O-C Gateway)	-
2447477.33300	-	Min I (visual)	Blaettler (O-C Gateway)	-
2447555.34200	-	Min I (visual)	Blaettler (O-C Gateway)	-
2447886.51900	-	Min I (visual)	Locher (O-C Gateway)	-
2448190.64300	-	Min I (visual)	Locher (O-C Gateway)	-
2448586.27300	-	Min I (visual)	Peter (O-C Gateway)	-
2450050.38500	-	Min I (visual)	Vandenbroere (O-C Gateway)	-
2451140.37300	-	Min I (visual)	Vandenbroere (O-C Gateway)	-
2451377.19800	-	Min I (CCD)	Paschke (O-C gateway)	-
2451525.24300	-	Min I (visual)	Vandenbroere (O-C Gateway)	-
2451576.36500	-	Min I (visual)	Verrot (O-C Gateway)	-
2451810.50570	0.00160	Min I (CCD)	BBSAG Bulletin (2000)	-

2451934.30200	-	Min I (visual)	Verrot (O-C Gateway)	-
2453253.08330	0.00054	Min I (CCD)	This study (WASP)	(a)
2453718.68590	0.00010	Min I (CCD)	Nelson (2006)	-
2453998.58716	0.00054	Min I (CCD)	This study (WASP)	(b)
2454006.66097	0.00039	Min I (CCD)	This study (WASP)	(b)
2454025.49989	0.00010	Min I (CCD)	Brát et al. (2009)	-
2454057.79725	0.00051	Min I (CCD)	This study (WASP)	(a)
2454087.40057	0.00117	Min I (CCD)	This study (WASP)	(b)
2454143.91780	-	Min I (CCD)	Nagai (2008)	-
2455161.23757	0.00168	Min I (CCD)	Zasche et al. (2011)	-
2455201.60720	0.00050	Min I (CCD)	Diethelm (2010)	-
2455535.33351	0.00050	Min I (CCD)	Brát et al. (2011)	-
2455777.55185	0.00050	Min I (CCD)	Hoňková et al. (2013)	-
2455844.83770	0.00090	Min I (CCD)	Diethelm (2012a)	-
2456210.85690	0.00030	Min I (CCD)	Diethelm (2012b)	-
2456638.77566	0.00510	Min I (CCD)	This study (KWS)	(a)
2456956.35670	0.00310	Min I (CCD)	This study (ASAS-SN)	(a)
2457287.39540	0.00250	Min I (Photoelectric)	Hübscher (2017)	-
2457343.91372	0.00065	Min I (CCD)	This study (ASAS-SN)	(a)
2457661.49395	0.00020	Min I (CCD)	Juryšek et al. (2017)	-
2457696.48275	0.00121	Min I (CCD)	This study (ASAS-SN)	(a)
2458070.57848	0.00094	Min I (CCD)	This study (ASAS-SN)	(a)
2458084.03869	0.00550	Min I (CCD)	This study (KWS)	(a)
2458439.29290	-	Min I (CCD)	Agerer (O-C gateway)	-

(a) These times of minima were derived using Zasche et al. (2014)'s method. (b) These times of minima were obtained from photometric observations directly.

Two different methods were used to calculate the minima times in this study. One of them is the Kwee-van Woerden method (Kwee & van Woerden 1956) by which the minima time calculated directly from observational data. Another method used is the Zasche et al. (2014)’s automatic fitting procedure. The method by which the minima times calculated in this study were mentioned in the last column of Table 3. The minima time data used in the period analysis covers the date range from August, 1936 to November, 2018.

In the O-C analysis of the system, MATLAB code given by Zasche et al. (2009) was used. In order to take into account the quality of the observational data, the minima times are weighted according to their types of observations. Accordingly, the minima times calculated from the observations made by visual (vis), photographic (pg), CCD and photoelectric (Pe) methods were weighted as 1, 5 and 10, respectively. The light element used in the analysis was taken from the study of Kreiner (2004). This light element is given below.

$$C_{1,\mathrm{TX\ Ari}} = \mathrm{HJD}\ 2452502.190 + 2^{\mathrm{d}}.691342\ \times E \quad (1)$$

O-C diagram of TX Ari is given in Figure 4.

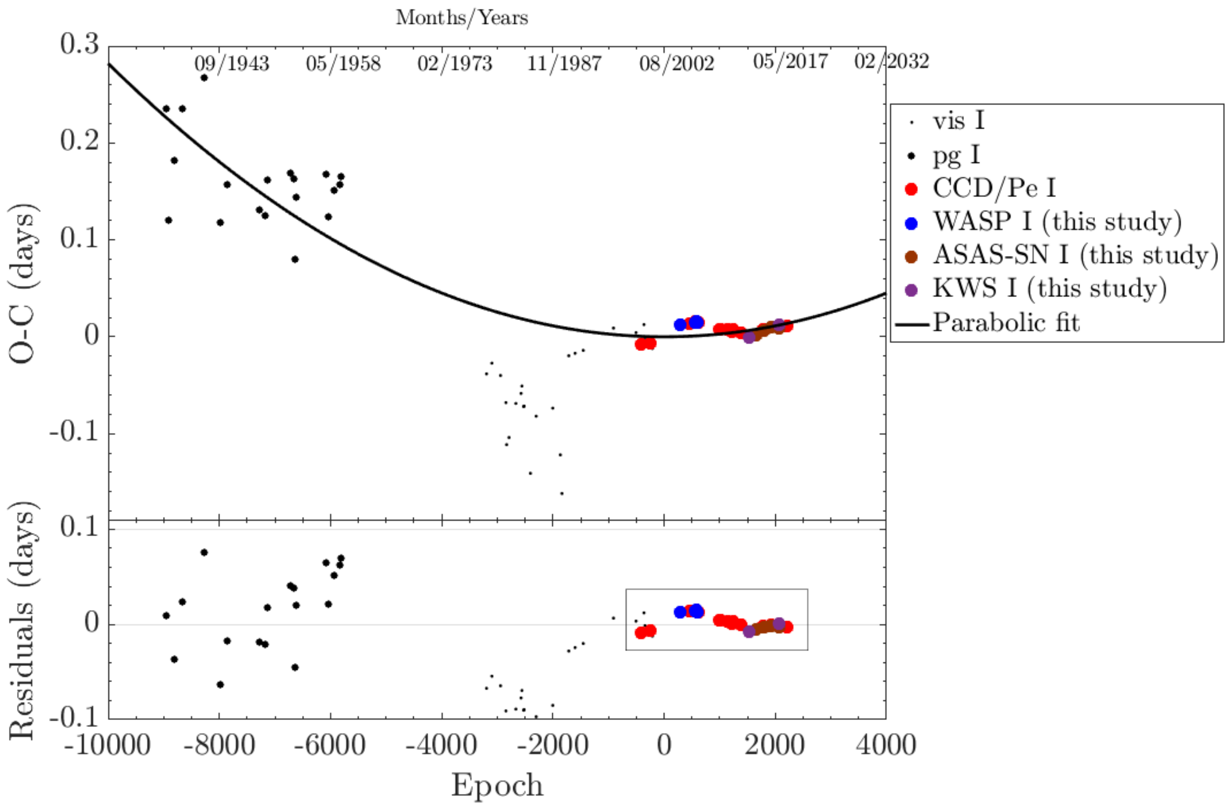

Figure 4. O-C diagram of TX Ari. Best parabolic fit to O-C dataset shown with solid black line. Residuals from parabolic fit shown in bottom part of diagram.

As can be seen from Figure 4, a parabolic change is seen in the O-C diagram of the system. The quadratic light element obtained as a result of the period analysis of the system was found as follows.

$$C_{2,\mathrm{TX\ Ari}} = \mathrm{HJD}\ 2452502.1869(99) + 2^{\mathrm{d}}.691340(2)\ \times E + 28^{\mathrm{d}}.20(6.81)\ \times 10^{-10} \times E^2 \quad (2)$$

According to the quadratic light element of the TX Ari system, the quadratic term was obtained as $28^{\mathrm{d}}.20(6.81)\ \times 10^{-10}$ days. Therefore, the orbital period of the system is secularly increasing with a rate of 0.066 ± 0.013 s/year. As mentioned in the light curve analysis section, the secondary component of the TX Ari system filled its Roche Lobe. Therefore, the upward parabolic change seen in the O-C diagram can be explained by the mass transfer mechanism from the secondary component to the primary component. This case is discussed in detail in the next section.

In the lower part of Figure 4, a cyclical change is noticeable only for CCD/Pe data, which is enclosed in a rectangle. Possible cause of cyclic O-C variation may be the light travel time effect (LTTE) due to a third body which is physically bound to the system. In order to examine this situation, the following LTTE equation given by Irwin (1959) was fitted to the O-C diagram of the system.

$$\Delta t = \frac{a_{12}\sin i_{12}}{c}\left\{\frac{1-e_{12}^2}{1+e_{12}\cos\nu_{12}}\sin(\nu_{12}+\omega_{12})+e_{12}\cos\omega_{12}\right\} \quad (3)$$

where Δt is the time advance/delay due to LTTE, c is the speed of light, and a_{12}, i_{12}, e_{12} and ω_{12} are the semi-major axis, inclination, eccentricity and longitude of the periastron of the absolute orbit of the center of mass of the eclipsing binary around the three-bod ysystem, respectively. ν_{12} is the true anomaly of the position of the eclipsing binary's mass center on this orbit and includes T_{12} and P_{12}, (the unseen/hidden parameters of Eq. (3), where T_{12} is the epoch of the passage at the periastron of the eclipsing binary's mass center along its orbit, and P_{12} is its orbital period).

The O-C diagram obtained as a result of the LTTE model is given in Figure 5. The parameter values obtained from the O-C analysis are given in Table 4. The term A' given in Table 4 gives the amplitude of the cyclical change, the term $f(M_3)$ gives the mass function of the third body, and the term M_3 gives the mass of the possible third body.

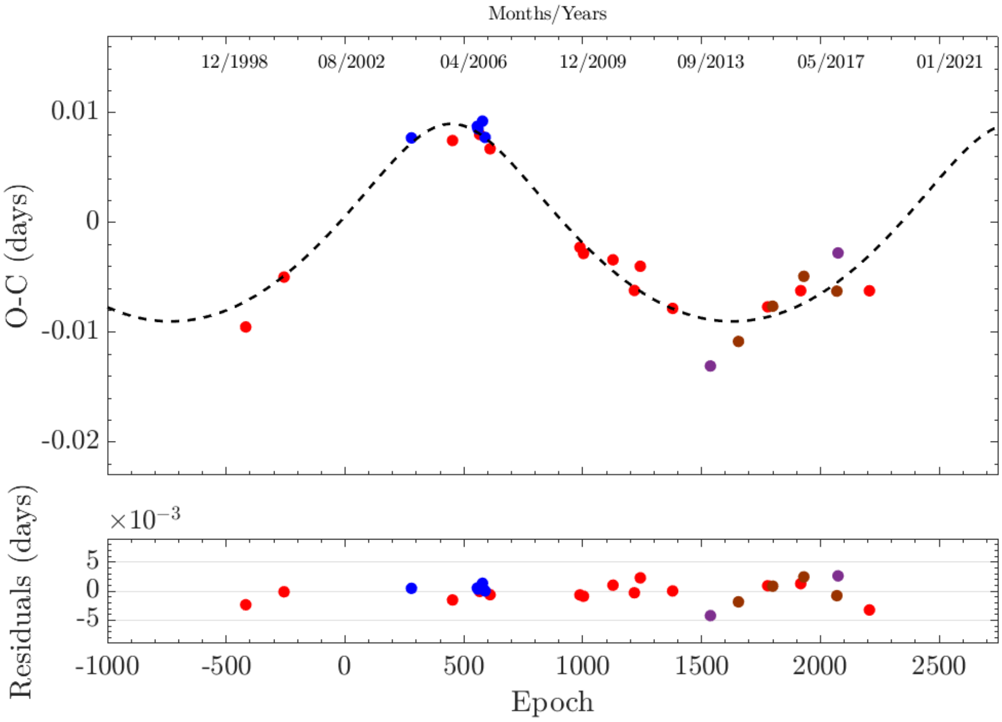

Figure 5. LTTE representation (solid black line) of O-C variation of TX Ari, and residuals from the best-fit curve.

Table 4. Parameters derived from O-C analysis of TX Ari.

Parameters	Value
T_0 (HJD)	2452502.1869±0.0099
P (days)	2.691340±0.000002
Q (10-10days)	28.20±6.81
A' (days)	0.0090±0.0012
$a_{12}\sin i_{12}$ (AU)	1.56±0.21
e_{12}	0.32±0.09
ω_{12} (deg)	90±12
P_{12} (years)	17.4±1.3
$f(M_3)$ (M⊙)	0.01249±0.00028
M_3 (M⊙) for $i_{12} = 30^0$	0.91±0.08
M_3 (M⊙) for $i_{12} = 60^0$	0.53±0.06
M_3 (M⊙) for $i_{12} = 90^0$	0.46±0.04
$\sum(O-C)^2$ (days^2)	0.0006

According to the parameters given in Table 4, TX Ari orbits around the triple system's center of mass in an eccentric orbit ($e_{12} = 0.32 \pm 0.09$) with a period of $P_{12} = 17.4 \pm 1.3$ years. The projected distance of the center of mass of TX Ari to the center of mass of the three-body system was estimated to be $a_{12}\sin i_{12}$=1.56±0.21 AU. Using the P_{12} and $a_{12}\sin i_{12}$ values, the mass function of the third body was found to be $f(M_3) = 0.01245 \pm 0.00028$ M⊙. More discussion on the LTTE effect is presented in the final section.

5. RESULTS AND DISCUSSIONS

Since there are no published radial velocity measurements of TX Ari, we estimated the absolute parameters, as given in Table 5. The mass of the primary component was estimated using the calibrations of the color index, effective temperature, mass and spectral type for main-sequence stars given by Drilling and Landolt (2000). We assumed a 10 per cent error in the estimated mass of the primary component in order to estimate the errors of the remaining parameters given in Table 5. The mass of the secondary component of TX Ari was calculated from the photometric mass ratio given in Table 2. The semi-major axes (A) were derived from Kepler's third law. Lastly, the bolometric magnitudes (M_{bol}) and surface gravity ($\log g$) values were estimated using the solar values ($T_{eff} = 5771.8 \pm 0.7$ K, $M_{bol} = 4.7554 \pm 0.0004$ mag, and $g = 27423.2 \pm 7.9$ cm/s^2) given by Pecaut and Mamajek (2013).

Table 5. Estimated absolute parameters of TX Ari

	Primary star	Secondary star
A (R⊙)	10.73 ± 0.21	
M (M⊙)	1.85 ± 0.19	0.44 ± 0.15
R (R⊙)	2.73 ± 0.19	3.07 ± 0.47
$\log g$ (cgs)	3.84 ± 0.09	3.11 ± 0.07
M_{bol} (mag)	1.24 ± 0.15	3.89 ± 0.51

As a result of the light curve analysis of the TX Ari (see Section 3), it was determined that the secondary component filled its Roche lobe. It is known that a fraction of the mass can be transferred to the more massive primary component when the less massive secondary fills its Roche lobe. In this case, the orbital period of the binary star system may show a periodic increase. In addition, a partial fraction of the mass can also be lost due to the magnetic braking effect of stellar winds, which give rise to a decrease in the orbital period of the binary system. Therefore, we considered the combined effect of mass transfer and mass loss from the system, i.e. a non-conservative mass transfer mechanism, to interpret the orbital period change of TX Ari. We used the equation given by Erdem & Öztürk (2014) in order to calculate the rate of mass transfer from the secondary component to primary component and the rate of mass loss from the system. The relation between the rate of orbital period change and the rate of mass transfer and loss in semi-detached binaries is given below by Erdem & Öztürk (2014):

$$\frac{\dot{P}}{P} = \left\{2\left\{\frac{10R_2}{A}\right\}^2 \frac{M_1 + M_2}{M_1 M_2} - \frac{2}{M_1 + M_2}\right\}\dot{M} + \frac{3(M_1 - M_2)}{M_1 + M_2}\dot{M}_1 \tag{4}$$

where $\dot{P}$ and $\dot{M}_1$ are the rate of orbital period change and the rate of transferred mass from the secondary to primary component, respectively. $\dot{M}$ represents the rate of mass loss from the system and is defined as below:

$$\dot{M} \leq (1 - \beta)\dot{M}_2 = \frac{(1 - \beta)}{\beta}\dot{M}_1 \tag{5}$$

$$\beta = -\frac{\dot{M}_1}{\dot{M}_2} \tag{6}$$

where $\dot{M}_2$ is the mass loss rate of the secondary component and β is the mass-loss parameter giving the fraction of mass lost by the secondary component that is accreted by the primary component.

According to the scenario presented by Erdem & Öztürk (2014), the mass transfer mechanism form secondary to primary component is the dominant mechanism and the orbital period of the binary system subsequently increases if the mass-loss parameter, β, is larger than its critical value, β_{cri}).

The critical value of the mass-loss parameter (β_{cri}) can be derived from Eqs. (4) and (5). The β_{cri} value of TX Ari was found to be 0.897. Therefore, the mass-loss parameter for the system should be in the range of $\beta_{cri} = 0.897 < \beta < 1$. The $\beta - \dot{M}_2$ diagram of the system is also given in Figure 6.

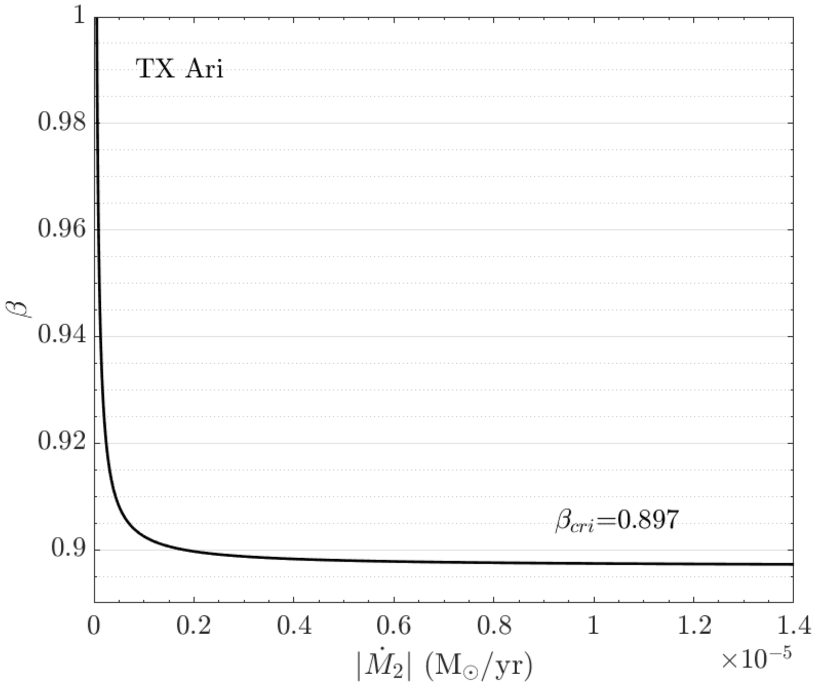

Figure 6. $\beta - \dot{M}_2$ diagram of TX Ari.

Using Eqs. (4) and (5) for $\beta \cong 0.897$, values of the mass transfer rate to the primary component ($\dot{M}_1$) and the mass-loss rate ($\dot{M}$) were found to be in the order of 10^{-6} M⊙/year and 10^{-7} M⊙/year, respectively. In case of conservative mass transfer mechanism, i.e. $\beta = 1$, the rate of transferred mass to the primary component is calculated to be in the order of 10^{-8} M⊙/year.

As mentioned in the previous section, a cyclical change was also observed in the O-C diagram of the system and this change was interpreted by the LTTE mechanism. According to the masses of the primary and secondary components of TX Ari given in Table 5, the mass of the hypothetical third body was found to be 0.91 (±0.08) M⊙, 0.53(±0.06) M⊙, and 0.46 (±0.04) M⊙ for $i_{12} = 30^0$, $i_{12} = 60^0$ and $i_{12} = 90^0$, respectively. If the third body is coplanar with the binary star system (i_{12} = i = $81^0.6$), see Table 2), then the mass and semi-major axis of its orbit around the center of the mass of the three-body system is derived to be 0.46(±0.05) M⊙ and 7.8(±1.2) AU. According to Allen's tables for main-sequence stars (Drilling and Landolt, 2000), if we assume that the third body is a main-sequence star then it should be a dwarf of early-M spectral type. The light contribution of the third body to the total light of the system was estimated to be ~ 0.09% using the mass– luminosity relation of $L \sim M^{3.9}$ given by Ibanoğlu et al. (2006). Therefore, the light contribution from the third body is too small to be observed photometrically.

In this study, a detailed photometric study of eclipsing binary systems TX Ari was given for the first time. High-resolution spectroscopic observations together with more precise photometric observations of the system are required in order to estimate the absolute parameters more reliably, to understand the nature of the long-term O-C variation.

REFERENCES

Andrae, R., Fouesneau, M., Creevey, O……. Bailer-Jones, C. A. L. (2018). Gaia Data Release 2. First stellar parameters from Apsis. Astronomy & Astrophysics, 616, id.A8.

BBSAG Bulletin (2000). 156. LIST OF MINIMA OF ECLIPSING BINARIES, BBSAG Bulletin, 123, 1-10.

Bradstreet, D. H., & Steelman, D. P. (2002). Binary Maker 3.0 - An Interactive Graphics-Based Light Curve Synthesis Program Written in Java. Bulletin of the American Astronomical Society, 34, 1224.

Brát, L., Trnka, J, Šmelcer, L……. Zambelli, R. (2011). B.R.N.O. Contributions #37 Times of minima, Open European Journal on Variable stars, 137, 1-57.

Brát, L., Trnka, J., Lehký, M……. Vítek, M. (2009). B.R.N.O. Contributions #36 Times of minima, Open European Journal on Variable stars, 107, 1-32.

Butters, O. W., West, R. G., Anderson, D. R……. Wilson, D. M. (2010). The first WASP public data release. Astronomy and Astrophysics, 520, id.L10.

Diethelm, R. (2010). TIMINGS OF MINIMA OF ECLIPSING BINARIES, Information Bulletin on Variable Stars, 5945, 1-9.

Diethelm, R. (2012a). TIMINGS OF MINIMA OF ECLIPSING BINARIES. Information Bulletin on Variable Stars, 6011, 1-13.

Diethelm, R. (2012b). TIMINGS OF MINIMA OF ECLIPSING BINARIES. Information Bulletin on Variable Stars, 6042, 1-10.

Drake, A. J., Djorgovski, S. G., Mahabal, A……. Kowalski, R. (2009). First Results from the Catalina Real-Time Transient Survey. The Astrophysical Journal, 696(1), 870–884.

Drilling, J. S., &Landolt, A. U. (2000). Normal Stars. Allen's astrophysical quantities, 4th ed. Edited by Arthur N. Cox. ISBN: 0-387-98746-0. Publisher: New York: AIP Press; Springer, p.381.

Erdem, A., & Öztürk, O. (2014). Non-conservative mass transfers in Algols. Monthly Notices of the Royal Astronomical Society, 441(2), 1166-1176.

Hoňková, K., Juryšek, J., Lehký, M……. Čaloud, J. (2013). B.R.N.O. Contributions #38 Times of minima. Open European Journal on Variable stars, 160, 1-174.

Hübscher, J. (2017). BAV-RESULTS OF OBSERVATIONS - PHOTOELECTRIC MINIMA OF SELECTED ECLIPSING BINARIES AND MAXIMA OF PULSATING STARS. Information Bulletin on Variable Stars, 6196, 1-27.

Ibanoğlu, C., Soydugan, F., Soydugan, E., Dervişoğlu, A. (2006). Angular momentum evolution of Algol binaries. Monthly Notices of the Royal Astronomical Society, 373(1), 435-448.

Juryšek, J., Hoňková, K., Šmelcer, L……. Ziková, A. (2017), B.R.N.O. Contributions #40 Times of minima. Open European Journal on Variable stars, 179, 1-145.

Kochanek, C. S., Shappee, B. J., Stanek, K. Z……. Pojmański, G. (2017). The All-Sky Automated Survey for Supernovae (ASAS-SN) Light Curve Server v1.0. Publications of the Astronomical Society of the Pacific, 129(980), id.104502.

Kreiner, J. M. (2004). Up-to-Date Linear Elements of Eclipsing Binaries. Acta Astronomica, 54, 207-210.

Kwee, K. K., & van Woerden, H. (1956).A method for computing accurately the epoch of minimum of an eclipsing variable. Bulletin of the Astronomical Institutes of the Netherlands, 12, 327-330.

Levine, S., Henden, A., Terrell, D., Welch, D., Kloppenborg, B. (2019) Solar System Objects and the AAVSO Photometric All-Sky Survey (APASS). The Journal of the American Association of Variable Star Observers, 47(1), 132.

Lucy, L.B. (1967). Gravity-Darkening for Stars with Convective Envelopes. Zeitschrift für Astrophysik, 65, 89–92.

Nagai, K. (2008). Visual and CCD minima of eclipsing binaries during 2007. Variable Star Bulletin 46 (1), 1-8.

Nelson, R. H. (2006). CCD MINIMA FOR SELECTED ECLIPSING BINARIES IN 2005, Information Bulletin on Variable Stars, 5672, 1-4.

Pecaut, M.J., & Mamajek, E.E. (2013). Intrinsic colors, temperatures, and bolometric corrections of pre-main-sequence stars. The Astrophysical Journal Supplement, 208 (1), id.9.

Ruciński, S.M. (1969). The Proximity Effects in Close Binary Systems. II. The Bolometric Reflection Effect for Stars with Deep Convective Envelopes. Acta Astronomica, 19, 245–255.

Samus', N. N., Kazarovets, E. V., Durlevich, O. V., Kireeva, N. N., & Pastukhova, E. N. (2017). General catalogue of variable stars: Version GCVS 5.1. Astronomy Reports, 61(1), 80-88.

Shappee, B. J., Prieto, J. L., Grupe, D……. Yoon, Y. (2014). The Man behind the Curtain: X-Rays Drive the UV through NIR Variability in the 2013 Active Galactic Nucleus Outburst in NGC 2617. The Astrophysical Journal, 788(1), id.48.

von Zeipel, H. (1924). The radiative equilibrium of a rotating system of gaseous masses. Monthly Notices of the Royal Astronomical Society, 84, 665-683.

Wilson, R.E. (2012). Spotted star light curves with enhanced precision. The Astronomical Journal, 144(3), id.73.

Wilson, R.E., & Devinney, E.J. (1971). Realization of Accurate Close-Binary Light Curves: Application to MR Cygni. Astrophysical Journal, 166, 605–619.

Woźniak, P. R., Vestrand, W. T., Akerlof, C. W……. Wren, J. (2004). Northern Sky Variability Survey: Public Data Release. The Astronomical Journal, 127(4), 2436–244.

Zasche, P, Uhlař, R., Kučaková, H. , Svoboda, P. (2011). COLLECTION OF MINIMA, Information Bulletin on Variable Stars, 6007, 1-12.

Zasche, P., Liakos, A., Niarchos, P., Wolf, M., Manimanis, V., Gazeas, K. (2009). Period changes in six contact binaries: WZ And, V803 Aql, DF Hya, PY Lyr, FZ Ori, and AH Tau. New Astronomy, 14(2), 121-128.

Zasche, P., Wolf, M., Vraštil, J., Liška, J., Skarka, M., Zejda, M. (2014). Apsidal motion and a light curve solution for eighteen SMC eccentric eclipsing binaries. Astronomy & Astrophysics, 572, idA71.